

## Wind Characteristics of Mesquite Streets in the Northern Chihuahuan Desert, New Mexico, USA\*

DALE A. GILLETTE<sup>a,\*</sup>, JEFF E. HERRICK<sup>b</sup> and GARY  
A. HERBERT<sup>c</sup>

<sup>a</sup>*Air Resources Laboratory, Air-Surface Processes Modeling Branch, National Oceanic and Atmospheric Administration, U. S. Department of Commerce, MD-81, Research Triangle Park, NC 27711, USA;* <sup>b</sup>*Jornada Experimental Station, US Department of Agriculture, Las Cruces, NM, USA;* <sup>c</sup>*G. A. Herbert Associates, Boulder, CO 80304, USA*

Received 24 August 2005; accepted in revised form 19 December 2005

**Abstract.** Past research has shown that the most important areas for active sand movement in the northern part of the Chihuahuan Desert are mesquite-dominated desert ecosystems possessing sandy soil texture. The most active sand movement in the mesquite-dominated ecosystems has been shown to take place on elongated bare soil patches referred to as “streets”. Aerodynamic properties of mesquite streets eroded by wind should be included in explaining how mesquite streets are more emissive sand sources than surrounding desert land. To understand the effects of wind properties, we measured them at two flat mesquite sites having highly similar soil textures but very different configurations of mesquite. The differences in wind properties at the two sites were caused by differences of size, orientation, and porosity of the mesquite, along with the presence of mesquite coppice dunes (sand dunes stabilized by mesquites growing in the dune and on its surface) found only at one of the two sites. Wind direction,  $u_*$  (friction velocity),  $z_0$  (aerodynamic roughness height) and  $D$  (zero plane displacement height) were estimated for 15-m tower and 3-m mast data. These aerodynamic data allowed us to distinguish five categories with differing potentials for sediment transport. Sediment transport for the five categories varied from unrestricted, free transport to virtually no transport caused by vegetation protection from wind forces. In addition, “steering” of winds below the level of the tops of mesquite bushes and coppice dunes allowed longer parallel wind durations and increased wind erosion for streets that aligned roughly SW–NE.

**Key words:** Chihuahuan desert, desert winds, desert vegetation, dunes, dust emissions, flow around and above roughness elements, friction velocity, sand transport, vegetation

\*U.S. Government right to retain a non-exclusive royalty-free licence in and to any copy-right is acknowledged.

\*Corresponding author, E-mail: gillette.dale@epa.gov

**Abbreviations:**

$D$  – zero plane displacement height;

USEPA – United States Environmental Protection;

LTERR – Long Term Ecological Research;

NOAA – National Oceanic and Atmospheric Administration;

$Ri$  – Gradient Richardson number;

SF – Steadiness Factor;

$u_*$  – friction velocity;

$z_0$  – aerodynamic roughness height.

**1. Introduction**

Gillette and Pitchford [1] described wind erosion in the northern Chihuahuan Desert as that represented by the Jornada Long Term Ecological Research (LTERR) project. The Jornada LTERR project is located about 30 km NE of Las Cruces, NM, between the Rio Grande River (to the west) and White Sands National Monument (to the east). Except for small areas of disturbance caused by humans, the Jornada study area is vegetated, although in many areas this vegetation is sparse and patchy. The most intense area of wind erosion occurs in natural areas with sandy soils and mesquite vegetation (*Prosopis glandulosa*). Another finding was that most of the sand transport in the mesquite-vegetated sandy soils occurred in elongated bare-soil areas referred to as streets that are oriented in the direction of the strongest winds. Streets were not observed for any of the other dominant vegetation species of the northern Chihuahuan Desert. Sand fluxes were observed to increase with downwind distance in streets that were oriented parallel to the wind direction. The mesquite bushes surrounding the sand-emitting streets in the Jornada study area had varying amounts of collected sand at their bases. The amount of this collected sand ranged from no sand to sand completely constituting the “body” of a mesquite-covered coppice dune. The mesquite present at one of our sites ranged in size from small single bushes to multiple large bushes incorporated into coppice dunes approximately 1.4 m high.

The aerodynamic effects of plants have been modeled, for example [2–7]. Additionally, the aerodynamic effects of sand dunes have been studied, for example, [8–11]. These studies have identified and described flow patterns as influenced by dunes.

We sought to identify wind characteristics for two flat mesquite-dominated sites that had similar soil properties. One of the sites had well-developed mesquite streets, whereas the other did not. The soil at the site without streets was shown by one of the authors (JH) to have an enriched calcium carbonate accumulation layer at depths of 30 to 50 cm that prevented root penetration below that level. Consequently, the mesquites at

this site consequently had stunted root growth leading to limited growth of the mesquite bushes above ground. The site with streets produced more wind-borne sand during wind storms. We sought to identify wind characteristics in and around the mesquite streets in similar categories, as was done for sand dunes by Walker and Nickling [11]. Our specific plan was the following:

*a. Characterize the surfaces.* Based on our observations at four Chihuahuan Desert mesquite-dominated sites [1, 12], we divided the surfaces of the two sites into two components each: bare, flat soil and roughness elements separated by the bare, flat soil. We characterized the surfaces so that differences between the two could be shown and for possible comparisons with future work. The bare, flat surface soil was characterized by measuring the soil particle size distributions. Size distribution of surface soil influences the threshold (minimum at which particle movement commences) friction velocity and source limitation of airborne particles. The “roughness elements” present on the sites were almost exclusively mesquite bushes and mesquite coppice dunes. Data on the mesquite bushes and coppice dunes consist of two-dimensional mapping of mesquite bushes/coppice dunes and bush and coppice dune heights. Optical porosity was used to approximate the penetrability of the mesquite bushes and mesquite coppice dunes by the wind. Raupach *et al.* [13] showed that for a given wind speed, penetration of wind into vegetation is related to optical porosity (the fraction of light passing through vegetation from diffuse white light). For a given wind speed, larger optical porosity correlates with more penetrable vegetation, that is, the smaller the penetrability (optical porosity), the more potentially disruptive the vegetation is on the flow patterns around the bushes and dunes. Therefore, the optical porosity of mesquite bushes or mesquite coppice dunes provides a qualitative index of whether wind goes through or around and over the mesquite.

*b. Measure wind directions and wind-direction variability at several points in the mesquite test sites during dust storms.* Gillette and Pitchford [1] found that the strongest sand-movement episodes had wind directions roughly in the same direction as the dominant mesquite bush/coppice dune orientation. We sought to test the hypothesis that our non-randomly situated mesquite bushes and mesquite coppice dunes act to steer the wind flow, thereby increasing the time during which wind blows parallel to long patches of flat, sandy soil.

*c. Measure wind-speed profiles and air-temperature profiles at both mesquite sites.* Wind-speed profiles were determined based on measurements at three to five heights for our nine wind-sampling points. Wind and temperature profiles were used to estimate the gradient Richardson number, a dimensionless number that expresses the stability of the atmosphere [14], and three wind-profile parameters: aerodynamic roughness height,  $z_0$ , zero plane

displacement height,  $D$ , and wind-friction velocity  $u_*$ . To appropriately estimate these parameters, care was taken to meet the assumption that the flow is not separated. Together, the  $u_*$ ,  $D$ , and  $z_0$  values were used to characterize the wind flow at the two sites.

Zero plane displacement height,  $D$ , larger than zero expresses a lifting of the boundary layer flow above the surface, i.e., a skimming flow. One example of non-zero  $D$  is "canopy flow" [15]. In canopy flow, winds below height  $D$  are weaker and less organized than winds above  $D$ . For our purposes, weak and incoherent flow is not important to wind-borne sediment movement; we therefore regard areas where  $D > 0$  to be unlikely source areas of wind-blown sand but probable deposition zones.

Aerodynamic roughness length ( $z_0$ ) relates to the geometric scale of roughness on the surface, and an increase of  $z_0$  caused by fixed roughness correlates with an increase of threshold friction velocity [16]. Finally, friction velocity,  $u_*$  is related to the momentum transport to the surface. Several authors including Bagnold [17] and Owen [18] have shown that wind erosion mass fluxes are functions of friction velocity and threshold friction velocity.

*d. Measure threshold friction velocities.* Threshold friction velocities were estimated to provide an important parameter needed by existing equations expressing sand transport by wind. Friction velocities may be calculated for 10-min periods by measuring wind profiles. By simultaneously measuring a quantity proportional to sand movement, Threshold friction velocity,  $u_{*t}$ , were estimated by plotting friction velocities versus the response of an instrument that responds to airborne sand grains;  $u_{*t}$  was that friction velocity where the mean instrumental response to airborne sand movement was larger than the instrumental noise. For sandy soil surfaces free of roughness elements larger than 2 mm, threshold friction velocity is dependent only on the size distribution of the surface soil, particle density, surface pressure, and the force of gravity [19]. However, when roughness elements are present that are larger than coarse sand grains, threshold velocity is also dependent on the aerodynamic roughness length [20].

## 2. Experimental Methods

We observed wind speeds and directions, surface properties, and sand movement at two locations in the area of the Jornada U. S. Department of Agriculture-Agricultural Research Service (USDA-ARS) Jornada Experimental Range (JER) dominated by mesquite. The two locations were separated by approximately 6 km and each was established in close proximity to long-term vegetation monitoring plots maintained by the Jornada Long Term Ecological Research (LTER) program. Our observations were conducted from April 1 to 30, 2003. Our strategy was to estimate  $u_*$ ,  $z_0$ ,

and  $D$ , wind direction, and wind speed at one common height at two distinct mesquite-dominated sites: one had well-defined streets with lengths exceeding 10 m, and another had similar soil, similar total area of bare soil, but lacked well-organized streets. A vegetation map of our “Oriented” site (originally named MNORT) is shown in Figure 1. Our comparison “Random” site (originally named MWELL) vegetation map is shown in Figure 2. These figures illustrate streets at “Oriented.” At “Random,” bush density is greater but bush size is smaller than at “Oriented.” As suggested by our names, the placement of the smaller bushes at “Random” is

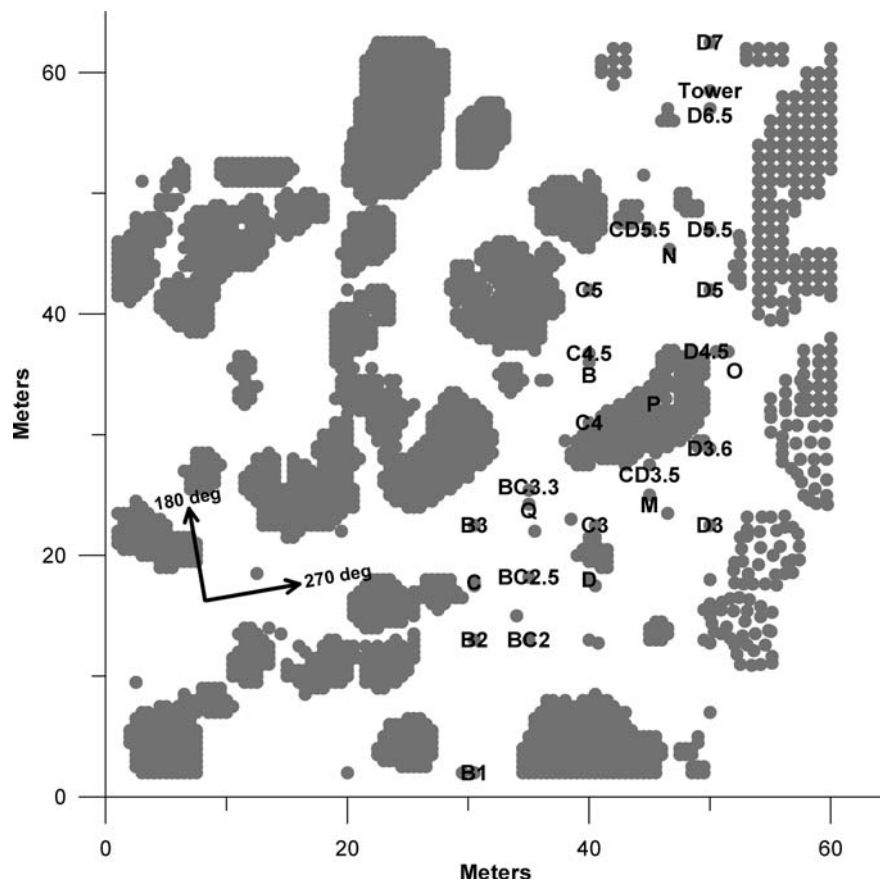


Figure 1. Map of locations at the “Oriented” site of mesquite plants (shown by shading), 15-m-high meteorological tower, eight 3-m-high masts and sand flux collectors. Sand flux collectors are labeled with a grid location using an alphabetical letter denoting a column, followed by a number denoting position in a row. The eight 3-m masts are denoted alphabetically  $B$ ,  $C$ ,  $D$ ,  $M$ ,  $N$ ,  $O$ ,  $P$ , and  $Q$ . The 15-m tower is labeled “tower.” Wind directions are shown as  $180^\circ$  (from the south) and  $270^\circ$  (from the west).

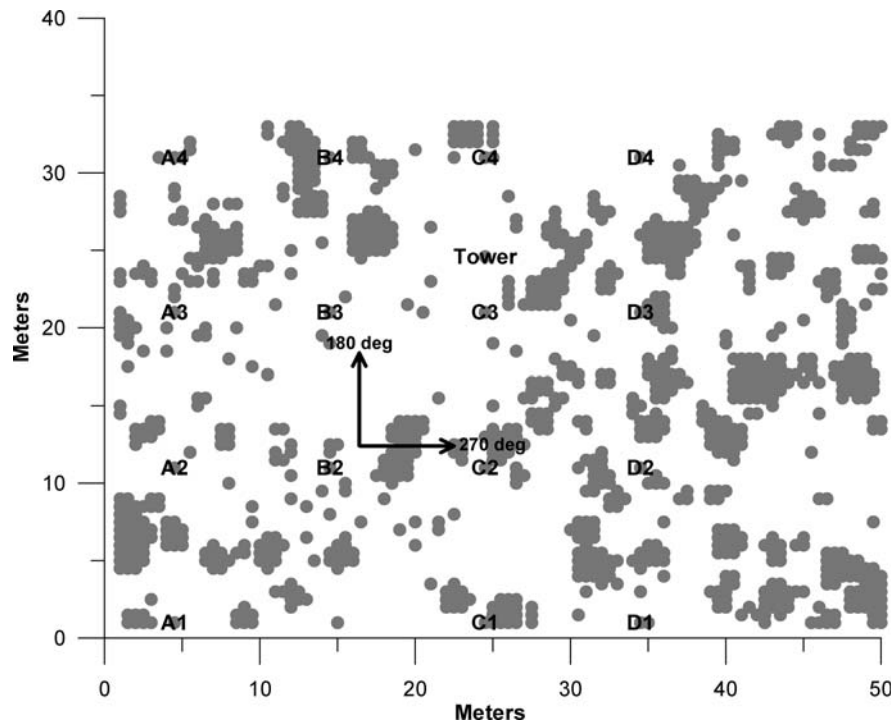


Figure 2. Map of locations at the “Random” site of mesquite plants (shown by shading), 15-m-high meteorological tower, and sand flux collectors. Sand flux collectors are labeled with a grid location using an alphabetical letter denoting a column, followed by a number denoting position in a row. The 15-m tower is labeled “tower.” Wind directions are shown as 180° (from the south) and 270° (from the west).

clearly different from the larger consolidated mesquite bushes and streets at “Oriented.” Larger mesquites were often associated with coppice dune development that had large volumes of sand within the volume of the mesquite bush. No large coppice dunes were found at “Random” and there was less trapping of sand by mesquite bushes than at “Oriented.” The more open and smaller mesquite bushes at “Random” would be expected to allow more wind through the plants compared to “Oriented” with less obstruction and steering of the wind.

At “Oriented” we used a 15-m tower at the end of a long street. The 3-m wind-profile masts were intentionally placed near mesquite bushes and coppice dunes. They were installed in the street areas of the “Oriented” site to investigate how local aerodynamic properties differ at locations characteristic of significant features of the site, specifically upwind and downwind of mesquite bushes and at midpoints on the streets. A 15-m tower was also installed at “Random” in a bare soil location near the center of the site.

The 15-m tower at “Oriented” had been in place since 2000; aerodynamic data obtained at this tower from 2000 to 2003 were used to provide a longer-time database for  $z_0$  and  $D$ . Eight 3-m masts were installed at “Oriented” for the April 2003 experiment. Both mesquite sites had single continuous Sensit<sup>TM</sup> sand flux monitoring devices built by the Sensit Co. of Portland, ND.<sup>1</sup>

Sand flux collectors were placed at “Oriented” and “Random.” The placements of the eight 3-m masts, the 15-m tower, the sand flux collectors, and the mesquite bushes are shown in Figure 1 for “Oriented” and Figure 2 for “Random.” In Figure 1, the shaded area within horizontal coordinates 38 to 50 m and vertical coordinates 25 to 38 m is called the “test dune.” This is a coppice dune formed by the trapping of moving sand by mesquite bushes. In both Figures 1 and 2, arrows point from the direction south ( $180^\circ$ ) and west ( $270^\circ$ ). The range of strong winds during April 2003 was roughly  $180^\circ$  to  $270^\circ$ . The mean and standard deviation of height of the mesquite plants from the soil level as well as vegetative cover (fraction of the ground covered by vegetation) measured by Gillette and Pitchford [1] are given in Table I.

## 2.1. METEOROLOGICAL PROFILE MEASUREMENTS AT THE MESQUITE STUDY SITES

Instrumentation for the 15-m tower at “Random” and “Oriented” sites are listed in Table II. For each 15-m tower, it consisted of five anemometers, two wind vanes, and two temperature sensors. Instrumentation for the 3-m masts was similar except there were no temperature sensors on the masts. Three-meter masts were not placed at “Random” because of the absence of long streets. Eight additional 3-m masts were used at the “Oriented” site to measure wind conditions in the bare areas of the two sites. Locations of the 3-m masts are shown in Figure 1 for “Oriented.” Since the study was not concerned with wind speeds lower than those that move sand, we used a system that only recorded 10-min average wind speeds larger than  $6 \text{ m s}^{-1}$ . Meteorological data were edited to eliminate questionable data caused by instrument problems.

Table I. Properties of the mesquite sites.

Property	“Oriented”	“Random”
Vegetative cover (%)	25.4	15.7
Mean Ht $\pm$ st. dev of bushes above soil (m)	$1.0 \pm 0.5$	$0.5 \pm 0.3$

Table II. Meteorological profile measurements at the mesquite study sites.

Location	Measurement type	Nom. Ht. of measurement (m)	Sampling frequency (/sec)	Averaging time (min)	Manufacturer
"Oriented" & "Random"	Wind speed	1.3	20	10	NRG Systems <sup>1</sup> 110 Commerce St. Hinesburg, VT
		2.6	20	10	
		3.8	20	10	
		7.5	20	10	
		15.0	20	10	
"Oriented" & "Random"	Wind direction	2.2	20	10	NRG Systems
		15.0	20	10	
"Oriented" & "Random"	Air temp	2.0	20	10	YSI Inc <sup>1</sup> , Yellow Springs, OH
		15.0	20	10	
"Oriented" 8 locations	Wind speed	0.75	20	10	NRG Systems, 110 Commerce St.
		1.5	20	10	
		3.0	20	10	

## 2.2. FAST-RESPONSE HORIZONTAL SAND MASS FLUX SENSORS

Fast-response horizontal mass flux Sensit<sup>TM</sup> sensors were placed at the two mesquite sites within five meters of the towers. Each omnidirectional Sensit<sup>TM</sup> sensor was set at a height of 5 cm above the ground surface. The sensor consists of a ring of piezoelectric material mounted on a steel cylinder 2.54 cm in diameter. It responds to particle impacts on the ring surface and converts the electrical responses to counts. These sensors have been used previously by Stockton and Gillette [21] to sense airborne sand movement. Sensit<sup>TM</sup> instrument responses were used to find threshold velocities; airborne sand fluxes operating at the same time as wind instrumentation marked the beginning of airborne sand movement. Gillette and Pitchford [1] reported that the Sensit<sup>TM</sup> instrument used in the present experiment provided output (counts) that was approximately proportional to sand flux experienced by the sensor.

## 2.3. CALCULATION OF AERODYNAMIC ROUGHNESS HEIGHT, ZERO PLANE DISPLACEMENT HEIGHT, FRICTION VELOCITY, AND RICHARDSON NUMBER

The methods used to compute friction velocity, zero-plane displacement height, and aerodynamic roughness length are given by Gillette *et al.* [22 and 23]. Equation (1) represents the wind profile for near-neutral atmospheric conditions:

$$U(z) = \frac{u_*}{k} \ln \left( \frac{z - D}{z_0} \right), \quad (1)$$

where  $U$  is wind speed at height  $z$ ,  $u_*$  is wind friction velocity,  $k$  is the von Karman constant (taken here to be 0.4),  $D$  is the zero plane displacement height and  $z_0$  is the aerodynamic roughness length.  $D$  is a relevant parameter for analysis of wind erosion. A non-zero displacement height indicates that the wind profile is lifted above the ground and consequently, smaller momentum flux than  $\rho u_*^2$  (where  $\rho$  is air density) would be expected for the surface [24]. Data at five heights to a maximum of 15 m were used to fit the parameters of Equation (1) by using the U.S. Environmental Protection Agency Fluid Modeling Facility algorithm LOGFIT. The program solves for the least-squares fit of  $U$  and  $\ln(z - D)$  where  $D$  is arbitrarily set to zero. The slope and the intercept  $U = 0$  of this line yield  $z_0$  and  $u_*$ . The program then iteratively increases  $D$  and searches for the value that gives the best fit. Three anemometers were used for each 3-m mast. Our estimations of wind-profile parameters used fixed points, the lowest of which is nominally 0.75 m (except for the mast on top of the mesquite coppice dune). In areas of abrupt changes of surface characteristics, the wind profile requires a minimum fetch (time  $\times$  propagation speed) from the roughness element to develop to the heights we sampled. Therefore, the boundary layers are still developing and changing; a source of error is the very non-homogeneity that we are trying to study.

### 2.3.1. *Fitting of Wind Data to Equation (1) and Errors*

In regions close to non-homogeneous roughness elements one can assume that aerodynamic interactions with the roughness elements will cause deviations from the logarithmic profile expressed in Equation (1). Deviations such as development of multiple internal boundary layers, for example would lead to errors by estimating only one set of parameters  $u_*$  and  $z_0$  to describe each profile. Our masts having only three levels of wind speed measurement could not provide enough data to estimate errors for Equation (1). However, our five-level mast was capable of minimally providing sufficient data to compute standard errors of the estimate for the fit of the 15 m tower wind data to Equation (1). Standard errors were calculated according the method of Miller and Freund [25].

### 2.3.2. *Errors Caused by Stability of the Atmosphere*

To express the stability of the atmosphere, we calculated the gradient Richardson number ( $Ri$ ) using Equation (2) [26] for every wind-profile measurement:

$$Ri = \frac{\left(\frac{g}{T}\right)\left(\gamma_d + \frac{\partial T}{\partial z}\right)}{(\partial U / \partial z)^2}. \quad (2)$$

Here  $g$  is the acceleration of gravity [ $\text{m s}^{-2}$ ],  $T$  is mean air temperature in degrees Kelvin, and  $\gamma_d$  is adiabatic lapse rate equal to a decrease of air temperature of  $9.8 \times 10^{-3} \text{ }^\circ\text{C}$  per meter of vertical height. Using expressions from Kaimal and Finnigan [27], factors to correct friction velocity for the effect of Richardson number are given in Equations (3) and (4) for conditions of large gradient of  $U$  with height.

$$\text{For } -2 < Ri < 0, \quad \text{Factor} = (1 + 16|Ri|)^{1/4} \quad (3)$$

$$\text{For } 0 < Ri < 1 \quad \text{Factor} = (1 + 5Ri)^{-1}, \quad (4)$$

where we have made the approximation that the gradient Richardson number is roughly equal to the flux Richardson number.

#### 2.4. COMPUTATION OF STEADINESS FACTOR (SF)

The Steadiness Factor [28] describes the variability of the wind direction measurement. The SF is the integer value of 100 times the ratio of the mean resultant wind speed to the mean scalar wind speed. An SF value of 100 would indicate no horizontal wind direction variability, but an SF value of 70 would indicate a very large horizontal wind direction variability.

Ten-minute mean vector and scalar wind speeds were calculated for approximately 1200 samples of wind speed and direction taken in the 10-min sampling period for each wind vane. At the end of the 10-min sampling period, we calculated (1) the mean scalar wind speed, (2) the mean vector wind speed, and (3) the SF.

#### 2.5. CUMULATED SEDIMENT FLUX MEASUREMENTS

Instrumentation and calculation of sand fluxes at the ‘‘Oriented’’ and ‘‘Random’’ sites were discussed in detail [1]. Big Spring Number Eight (BSNE) sand flux collectors were set in a 10-m-square grid pattern at the mesquite sites to estimate means for the inhomogeneous sand fluxes. For the present experiment, several BSNE sand collectors were added to take samples in areas of the ‘‘Oriented’’ site where aerodynamic properties were measured. These collectors were placed near the 3-m masts imbedded in mesquite vegetation on the ‘‘test dune’’ (near the  $P$  mast), behind the mesquite ‘‘test dune’’ (near the  $O$  mast), at the upwind nose of the dune (near the  $Q$  mast), at the midpoint of the southern boundary of the dune (near the  $M$  mast), upwind and south of the ‘‘test dune’’ (at the  $C$  mast), and in the street north of the dune (near the  $B$  and  $N$  masts) and in the street south of the dune (near the  $D$  mast).

## 2.6. SURFACE SOIL PROPERTIES

To support our assumption that the soils of the “Oriented” and “Random” locations were similar, we took soil samples at the two sites in December 2003. Soil samples were collected at a distance of 3 and 15 m on transects radiating at 0, 120, and 240 degree angles from each 15-m tower. At each sampling location, samples were removed from three depths: (a) a surface sample was obtained using a small vacuum cleaner over a 33 cm × 17 cm area, (b) three 0–5-mm-deep samples were collected with a flat 12-cm square shovel with 5 mm shoulders, and (c) three 5–20-mm-deep samples were collected with a soil core sampler having a 6.2 cm diameter. The three samples at the 0–5 and 5–20-mm depths were composited for analysis. Sand-silt-clay distributions were obtained using the hydrometer method [29]. Sand and silt are distinguished at a particle size of 50  $\mu\text{m}$ , and silt and clay are separated at a particle size of 2  $\mu\text{m}$ . The sand fraction was further analyzed with sieves that yielded size fractions of the sand at size limits of 1000, 500, 250, 106, and 53  $\mu\text{m}$ . Comparisons of the means of the fraction of mass within the size limits were made by using the *t*-test [25].

## 2.7. OPTICAL POROSITY

To determine a rough measure of the penetrability of the mesquites, optical porosity was measured using the method described by Grant and Nickling [6]. In this method, a photograph is taken against a white sheet illuminated from behind by the sun. The photograph is then digitized, and black (vegetation) and white (void) areas are counted. This visual porosity was simply a ratio of the number of white pixels to the total number of pixels for the area within the boundaries of the plant. Optical porosities were measured in summer 1999, when the leaves were fully expanded. For coppice dunes, a large part of the surface area measured covered a solid sand dune. Consequently, for the coppice dunes, optical porosity values were generally quite low.

# 3. Results

## 3.1. SIZE DISTRIBUTION OF SURFACE SOILS

Table III shows that the soils of both the “Oriented” and “Random” are very similar ( $p \geq 0.1$  for all fractions and depths; *t*-test,  $n = 6$ ). Large portions of the mass of both soils were in particles with diameters between 250 and 500  $\mu\text{m}$ . Both soils are classified as “sand” by the USDA system [30].

## 3.2. OPTICAL POROSITY MEASUREMENTS

The frontal area of mesquite was measured along with optical porosity for each optical porosity sample. By weighting the measured optical porosity by frontal

Table III. Mean percentage soil mass between size classes for two sites at three depths.

	Percent soil mass between sizes						
	V. coarse sand	Coarse sand	Medium sand	Fine sand	Very fine sand	Silt	Clay
"Oriented"							
	1–2 mm	0.5–1 mm	250–500 $\mu\text{m}$	106–250 $\mu\text{m}$	50–106 $\mu\text{m}$	2–50 $\mu\text{m}$	< 2 $\mu\text{m}$
Surface	3.9	17.4	40.1	29.7	4.7	1.5	2.4
0–5 mm	1.6	9.2	32.6	35.7	8.5	6.1	4.6
5–20 mm	1.1	6.9	31.7	37.4	8.6	6.7	5.0
"Random"							
Surface	1.5	15.0	41.3	32.3	4.7	1.5	3.3
0–5 mm	0.8	8.2	33.4	39.2	8.3	4.5	4.6
5–20 mm	0.8	7.5	33.1	39.6	8.6	4.9	4.3

projected area after defining a perimeter around the mesquite, the mean optical porosities for "Oriented" and "Random" were 8.0% and 17.3%, respectively. Unweighted-mean optical porosity for "Random" mesquites was 17.1% with a standard deviation of 4.2%. The frontal projected areas of the sampled mesquites at "Random" were all smaller than 3 m<sup>2</sup>. The mean optical porosity of "Oriented" mesquites for frontal areas smaller than 3 m<sup>2</sup> was 8.9% with 4.3% standard deviation. For a frontal area larger than 3 m<sup>2</sup> mean optical porosity was 5.1% with 2.7% standard deviation.

### 3.3. SOIL MOVEMENT NEAR THE 15-M TOWER VERSUS WIND DIRECTION

For the month of April 2003, 10-min-averaged measurements of both wind direction and Sensit<sup>TM</sup> response to the sand flux at 5-cm height provided us with a surrogate for sand flux versus wind measurements. Figures 3a and 3b show that for the month of April 2003 all the sand flux occurred when 15-m winds were from directions between 220 and 280 degrees at "Oriented" and between 240 and 300 degrees at "Random"; that is, there was a displacement of about 20° in the wind directions activating wind erosion at the two sites. Figure 3b compares favorably to a "sand rose" using wind data and a threshold velocity for wind erosion for the Geomet site located several kilometers to the south of our "Oriented" and "Random" test sites [31].

### 3.4. FITTING OF WIND DATA TO EQUATION (1) AND ERRORS

The mean relative standard error of the estimate for the fit of the 15 m tower wind data to Equation (1) was 3% ± 1% for all the wind measurements. The

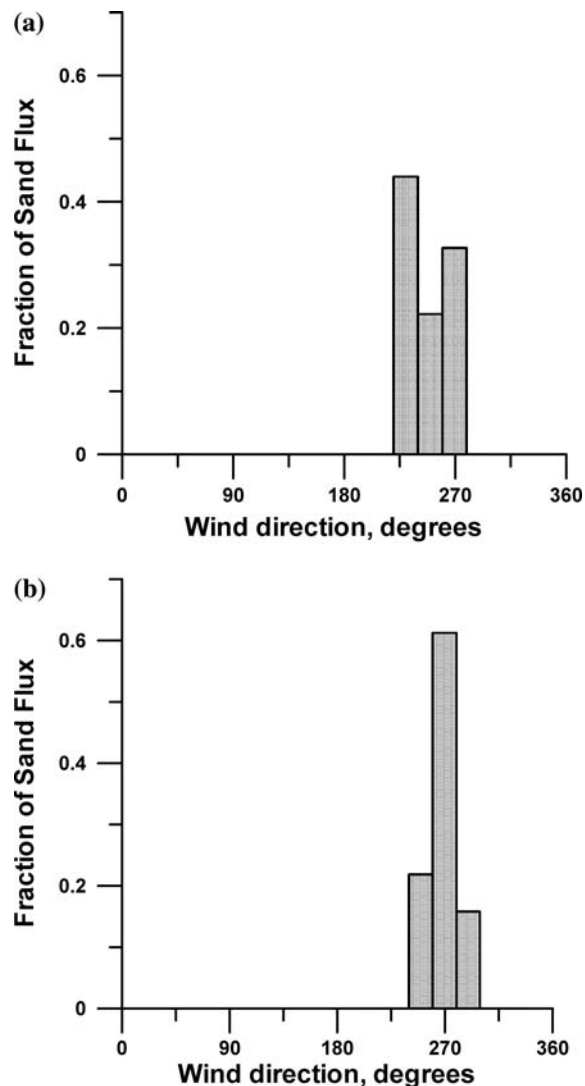


Figure 3. Wind direction, in degrees, versus the fraction of accumulated sand mass flux for the month of April 2003. (a). For "Oriented," (b). For "Random."

maximum standard error for 518 sets of fittings was 7% and the minimum standard error was 0.2%. We calculated the sample correlation coefficient squared ( $R^2$ ) to evaluate the quality of fit for the 3-m masts. The mean  $R^2$  values were 0.98 for the *B*, *C*, and *P* masts, 0.97 for the *D* mast, 0.92 for the *M* mast, 0.90 for the *N* mast, and 0.86 for the *Q* mast. Standard deviations for the mean  $R^2$  values for the masts ranged from 0.01 to 0.04. The fitting was not applied to wind data from the *O* mast because the observed separated flow at the mast made the fit invalid.

For our discussion of  $D$  and  $z_0$ , we restricted data to  $-0.075 < Ri < +0.01$ . The largest errors for our friction velocities caused by non-neutrality would be 22%. The errors for  $D$  and  $z_0$  caused by non neutrality would be larger. Our use of the profile data was to specify areas for which  $D = 0$  or  $D \neq 0$  and to specify the relative size of  $z_0$  values in the two area classes. Because we were only looking at relative sizes of  $z_0$  values, systematic errors in the  $z_0$  data would be compensated for by changing our definition of our boundary between “small” and “large”  $z_0$ . Errors in the profile data could also change the number of profiles for which  $D = 0$ . We estimate for all our measurement sites that the largest errors were caused by nonhomogeneous roughness rather than by non-neutral atmospheric conditions. Acknowledging the above errors, our analysis of the  $D$ ,  $z_0$ ,  $u_*$  and  $u_{*t}$  data will focus only on large differences and obvious trends.

Our data were only for relatively high winds (greater than  $6 \text{ m s}^{-1}$ ); almost all of these winds had directions between South and West. Although the possibility that the structure of the wind could show the effect of inhomogeneous upwind roughness elements, we interpret our data (mean standard error for fitting to Equation 1 of 3% and maximum of 7% for the 15-m tower) as showing that the wind profiles were close to being logarithmic and that the fit to Equation (1) furnishes values of  $D$ ,  $z_0$ ,  $u_*$  and  $u_{*t}$  that may be examined for large differences and obvious trends. Although we had no estimates of standard error of fit to Equation (1) for the 3-m masts data, the  $R^2$  values for Equation (1) for all the mast data except that for the  $O$  mast suggested to us that the values of  $D$ ,  $z_0$ ,  $u_*$  and  $u_{*t}$  that only apply to the lowest 3-m layer may likewise be examined for large differences and obvious trends.

### 3.5. THRESHOLD FRICTION VELOCITY MEASUREMENT

Threshold friction velocity was determined by plotting Sensit<sup>TM</sup> sand flux sensor output versus best-fit friction velocities from simultaneous 15-m tower wind measurements [12]. We designated threshold friction velocities,  $u_{*t}$ , as the intercept of zero sand flux and observed friction velocity. Figures 4a and 4b were interpreted so that “Oriented” and “Random” have the same threshold friction velocity:  $100 \text{ cm s}^{-1}$ . The threshold friction velocity,  $u_{*t}$ , for the “scrape site”, which was approximately 5 km to the south of the “Oriented” site and possessed highly similar soil to the “Oriented” and “Random” sites but was devoid of any vegetation, was  $25 \text{ cm s}^{-1}$  [12]. We interpreted the difference of threshold friction velocities at “Oriented” and “Random” sites compared to the “scrape site” as showing that 6% of the wind’s vertical momentum flux  $[u_{*t}(\text{scrape site})/u_{*t}(\text{“Oriented” or “Random”})]^2$  was being absorbed by the saltating sand particles, and 94% of the vertical momentum flux was being absorbed by the vegetation and dunes of the “Oriented” or “Random” sites. This interpretation uses Owen’s [18]

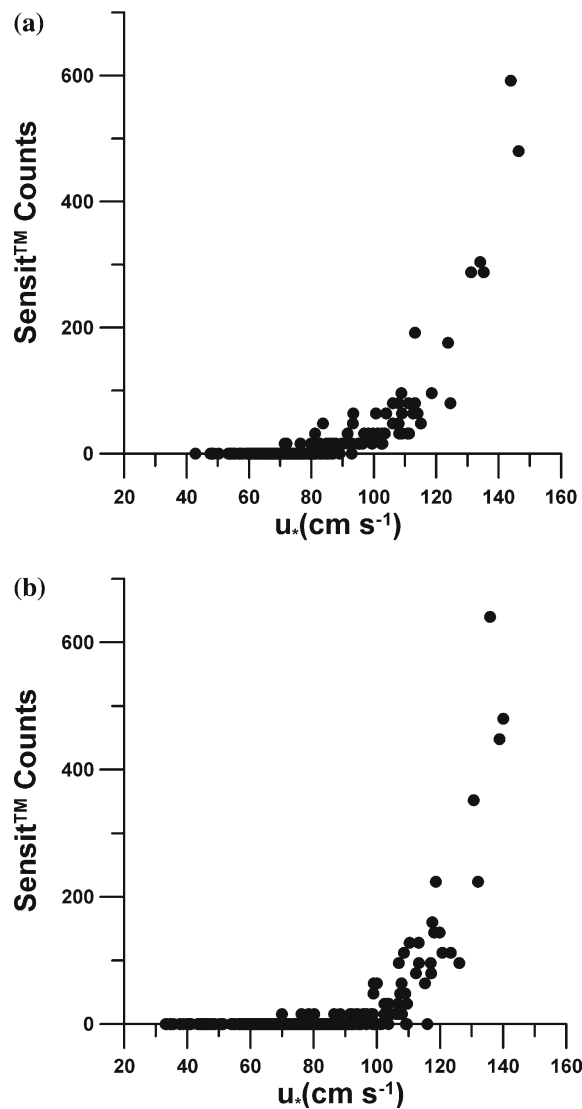


Figure 4. Sensit™ response to moving sand grains versus friction velocity. The intercept of the friction velocity with zero response is the threshold friction velocity. (a). For “Oriented,” (b). For “Random.”

theory that the vertical momentum flux of the wind is fully carried by saltating sand grains in the layer just above ground surface.

### 3.6. MEAN WIND SPEED AT 3.15 M HEIGHT FOR MATCHED GROUPS OF MASTS AT “ORIENTED”

The top anemometers of the eight masts at “Oriented” were taller (3.15 m) than any of the mesquite vegetation which approached 2 m on coppice

dunes. The wind flows at 3.15 m for the eight 3-m masts were above all roughness elements but not out of the aerodynamic influence of the underlying coppice dunes and mesquite bushes. Mean wind speed for masts initiated at the same time and stopped at the same time were compared for two groups of four masts. The two groups were masts *B, C, D,* and *M* and masts *N, O, P,* and *Q*. Mean and standard deviation of the mast wind speeds for the month of April 2003 were used to give a coefficient of variation (standard deviation divided by mean) for the two groups. For the group of masts *B, C, D,* and *M*, the coefficient of variation was 0.03, and for the group of masts *N, O, P,* and *Q*, it was 0.04. These coefficients of variations show that the mean wind speed at a height of 3.15 m above the ground was rather uniform for "Oriented," although possessing small variations.

### 3.7. STEERING OF WIND DIRECTION AT 1.5-M HEIGHT AT VARIOUS LOCATIONS IN THE "ORIENTED" COMPARED TO THE WIND DIRECTION AT 15-M HEIGHT ON THE "ORIENTED" TOWER

The steering effects of oriented coppice dunes were confirmed as variations of wind directions at a height of 1.5 m for eight masts at our "Oriented" site compared to a wind direction at 15-m. Although the mean height of all mesquite plants was one meter, heights of several of the mesquites exceeded 1.5 m when they were associated with coppice dunes. Comparisons of 1.5-m wind direction data with that for the 15-m tower wind direction for all the wind erosion events for April 2003 are shown in Figure 5. Each sub-figure of Figure 5 has an arrow that shows the approximate position of the 15-m tower and the individual 3-m mast (with wind vane height of 1.5 m) relative to the location of the "test dune." For a more accurate location of the masts, 15-m tower, and test dune, see Figure 1. Our interpretation of the data shown in Figure 5 follows from the distance relative to the dune height for the eight mast positions.

- (1) *Masts B and Q.* The largest steering observed was for masts *B* and *Q*. Clockwise steering is largest for south winds ( $180^\circ$  for the 15-m tower). For increasing wind direction, the steering slowly decreases to almost  $0^\circ$  at  $280^\circ$ . We attribute clockwise steering for 15-m wind directions greater than  $240^\circ$  to (1) the closeness of the "nose" of the test dune (just east of *Q*), which acts to divert air around this part of the dune, and (2) the separation of the boundary layer upwind of *B* at the downwind boundary of the high dune west of *B* for wind directions greater than  $240^\circ$  measured by the 15-m tower.
- (2) *Masts C and D.* These masts display maximum steering at  $180^\circ$  in common with masts *B* and *Q* with an approximately linear decrease of steering with increasing tower wind direction until both tower and mast wind directions are the same at about  $260^\circ$ . For 15-m wind directions

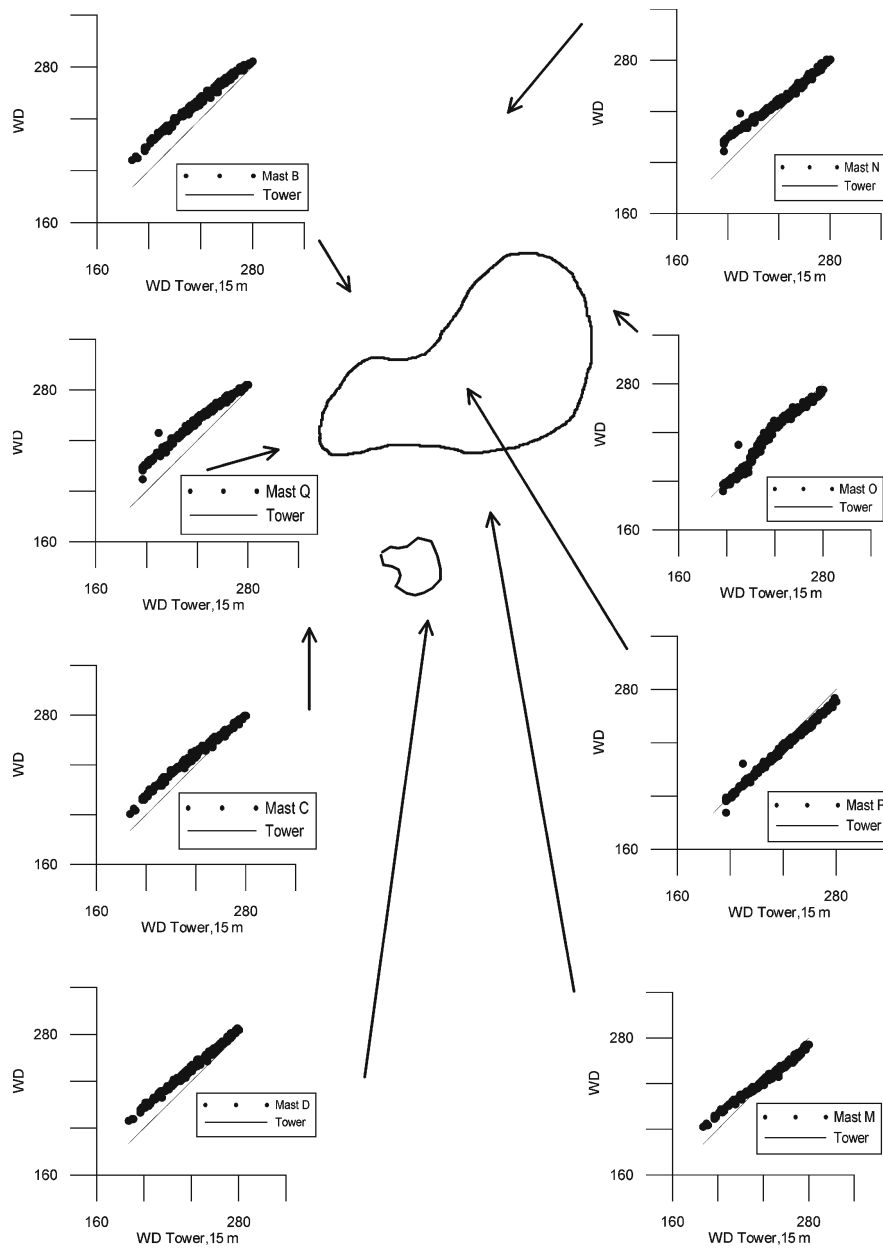


Figure 5. Comparison of wind direction from the 15-m tower wind vane (at 15-m height) and wind direction at 1.5-m height from the “Oriented” 3-m masts. Positions of masts relative to test dune are shown by arrow. Combined data for April 2003 were used. Masts shown: *B, N, Q, C, D, M, P, O.*

larger than  $260^\circ$ , mast and 15-m tower wind directions are close for up to  $280^\circ$ . For this range of directions, Masts *C* and *D* are influenced by dunes roughly lying west-east; south winds are steered clockwise but west winds are not.

- (3) *Masts M and N*. Masts *M* and *N* are located upwind of southwest-northeast lying dunes. For west winds, dunes to the south of *M* are parallel to the 15-m wind direction and do not steer the wind at *M*. Also, for west winds, mast *N* is downwind of short mesquite bushes. Steering by short bushes is expected to be minimal.
- (4) *Top of the test dune (Mast P)*. Figure 5 shows that the wind direction at 1.5-m height above the level of the top of the dune (approximately 1.5 m for a total height of the wind vane of approximately 3 m) is consistent with the wind direction at 15 m. This would be expected since there are no roughness elements higher than approximately 2 m.
- (5) *Downwind of the test dune (Mast O)*. Figure 5 shows that the 1.5-m-high wind direction east of the dune roughly follows the wind direction at 15 m. However, the wind direction trace shows more variability than that at Mast *P*. Observations during several storms in 2003 by the authors (not recorded electronically) were that winds at Mast *O* for height 5 cm to 20 cm were directed toward the back of the dune—almost opposite to those of the winds at 1.5-m height which were directed away from the back of the dune. Additionally, the wind direction was much more variable at 1.5 m than at any other mast even though the mean direction roughly follows the 15 m wind direction. This wind variability is consistent with the separation flow discussed by Walker and Nickling [11].

### 3.8. STEADINESS FACTORS (SF) VERSUS WIND DIRECTION

Figure 6 shows the Steadiness Factors developed for the wind vanes located on the 15-m-high tower (2.2-m and 15-m high) and the eight 1.5-m wind vanes on the masts, the locations of which are shown in Figure 1. The SF values were almost always larger than 90% for the 15-m-high wind vane and Masts *B*, *C*, *D*, *M*, *N*, *P* and *Q*. The 2.2-m wind vane on the tower produced very low values of SF for wind directions from  $190^\circ$  to  $200^\circ$  when the lower part of the tower was downwind of nearby mesquite coppice dunes but otherwise produced values larger than 0.9 for wind directions from  $200^\circ$  to  $280^\circ$ . For Mast *O* (downwind of the test dune for winds of  $230^\circ$ ) low SF values correspond to the observed flow separation and reversal of wind direction between heights just above the ground and about 1 m above the ground. Low SF values correlated with disturbed flow originating from nearly upwind mesquite bushes or mesquite coppice dunes. However, more distant upwind mesquite bushes or mesquite coppice bushes resulted in SF values larger than 90% (weaker disturbances).

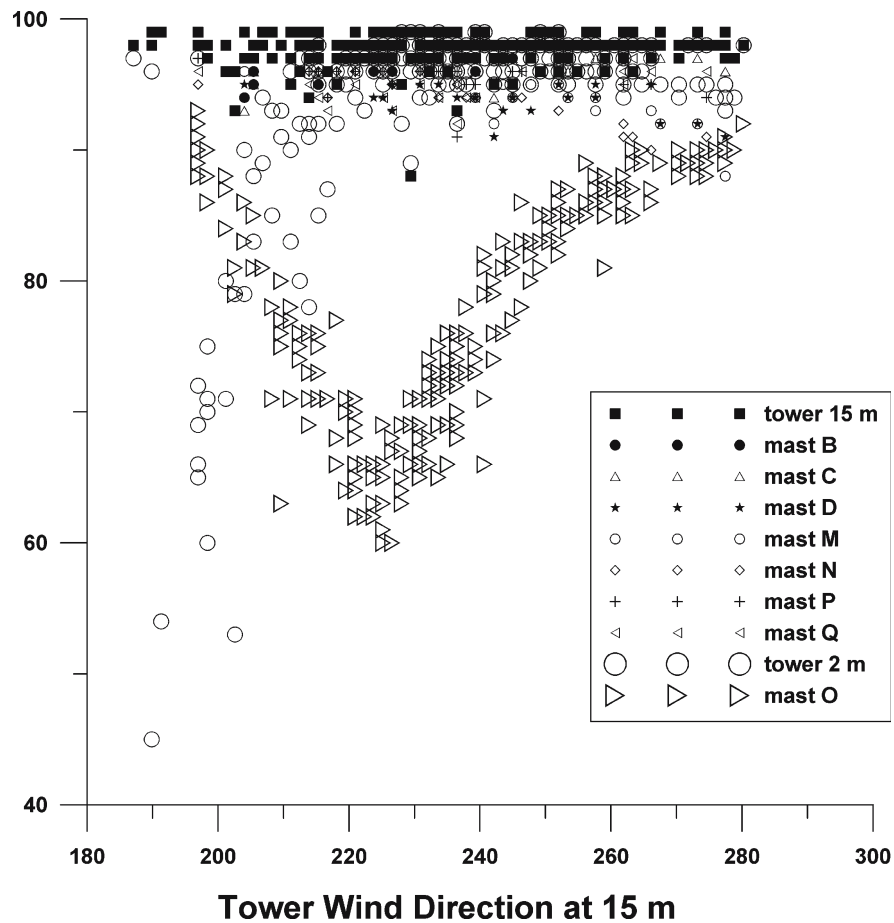


Figure 6. Steadiness Factor (SF) versus wind direction at 15-m.

### 3.9. “ORIENTED”: $D$ AND $Z_0$

#### 3.9.1. $D$ Versus $Sensit^T$ Response at the 15-m Tower

Figure 7 shows the  $Sensit^T$  response for the 15-m tower at our “Oriented” site for data taken in April 2003. For these data  $-0.075 < Ri < +0.01$ . These data show that there is a positive response at this site *only for*  $D=0$ . We have used this relationship to predict a necessary condition for sand flow at the “Oriented” site, which is that  $D=0$ .

#### 3.9.2. $D$ and $z_0$ Versus Wind Direction at the 15-m Tower

Composited data from 1999 to 2002 period and the April 2003 period at the “Oriented” 15-m tower site are shown for relationships of  $z_0$  and  $D$  versus wind direction at 15-m in Figures 8a and 8b. We used 15-m tower wind data for the period 1999–2002 to supplement the April 2003 data because it did not contain any 15-m wind directions from  $0^\circ$  to  $180^\circ$  or

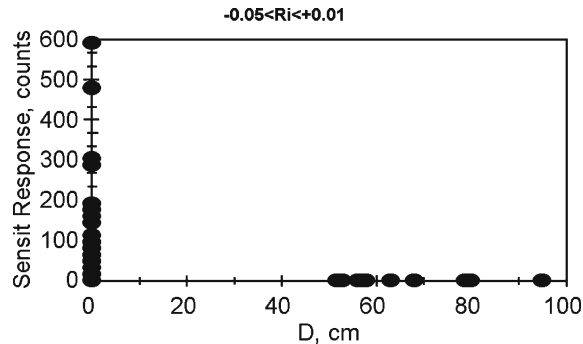


Figure 7. Sensit vs.  $D$  for the “Oriented” site. Note that no active sand movement was observed when  $D$  was not zero.

from  $290^\circ$  to  $360^\circ$ . For these data  $-0.075 < Ri < +0.01$ . The data set containing data for the full  $360^\circ$  of wind direction was needed to show relationships of  $z_0$  and  $D$  versus distance downwind of mesquite coppice dunes. The relationship of  $D$  versus wind direction at the 15-m tower (Figure 8a) shows that  $D$  is zero for all directions from  $200^\circ$  to  $360^\circ$ ; however, for the directions between  $100^\circ$  to  $200^\circ$ ,  $D$  values fluctuate randomly from 0 to 40 cm between these two wind directions. For these directions, the tower was less than 20 m downwind of mesquite bushes. For the wind direction range of  $124^\circ$ – $192^\circ$ , the tower was directly downwind of a 1.8-m-high mesquite coppice dune. For the wind direction  $159^\circ$  the downwind distance was 6.2 m. Sporadic non-zero  $D$ s at a given wind direction were interpreted to be caused by wake flow through, around, and over the nearby mesquite bushes.

Values of 15-m “Oriented” tower  $z_0$  shown in Figure 8b have a relation with wind direction. Since the 15-m “Oriented” tower was placed in a bare-soil area in inhomogeneous vegetation, the relationship of the  $z_0$  and  $D$  versus wind direction was unique to the placement of the tower. At  $114^\circ$ , the five anemometers were experiencing the wake flow from the tower itself, since the anemometers were located on 1-m-long arms, directly downwind of the tower shaft for this wind direction. Therefore, the  $D$  and  $z_0$  values at  $114^\circ$  should be disregarded. Upwind bush effects are seen in larger  $z_0$  values, for example from  $304^\circ$  to  $326^\circ$ ,  $24^\circ$  to  $47^\circ$ ,  $126^\circ$  to  $206^\circ$  and  $244^\circ$  to  $286^\circ$ .

The street upwind of the tower was aligned with the tower and Sensit<sup>TM</sup> instrument for the direction range  $232^\circ \pm 5^\circ$ , the primary wind direction during the storm. For this direction range and for  $D=0$  and  $z_0 < 15$  cm, the Sensit<sup>TM</sup> instrument showed maximum response. Sand flux appeared to reach optimal conditions when (1)  $D=0$  (See section 3.9.1) and (2)  $z_0 < 15$  cm (3)  $u_* > 100$  cm  $s^{-1}$  (that is, when friction velocity exceeded threshold value (see Figure 4a).

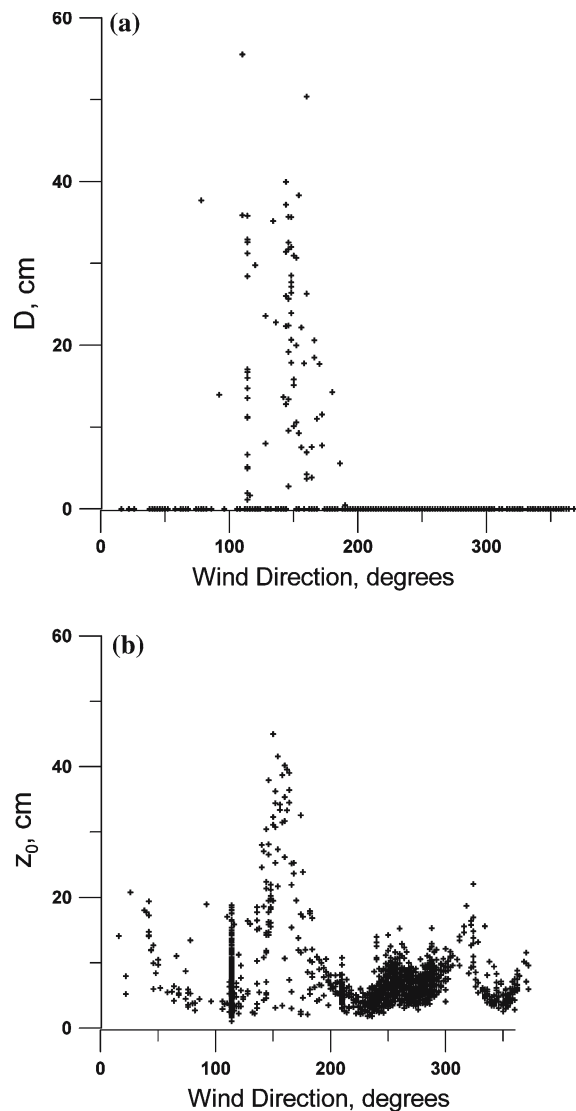


Figure 8. Data from 1999 through 2002 and the month of April 2003 versus wind direction at 15 m height of the “Oriented” tower. (a) Zero-plane displacement height  $D$ . (b) Aerodynamic roughness height  $z_0$ .

### 3.9.3. Relationship of $D$ to Distance to Nearby Mesquite Bushes and Bush Height

$D$  is related to the distance downwind from the nearest mesquite bush and depends on the height of the bush (Figure 9). Data for this site were used for this analysis because the “Oriented” site possessed ranges of wind speed for which  $D$  was always zero. In general the data suggest that  $D = 0$  if the distance is greater than 10 times the height of the upwind bush. This

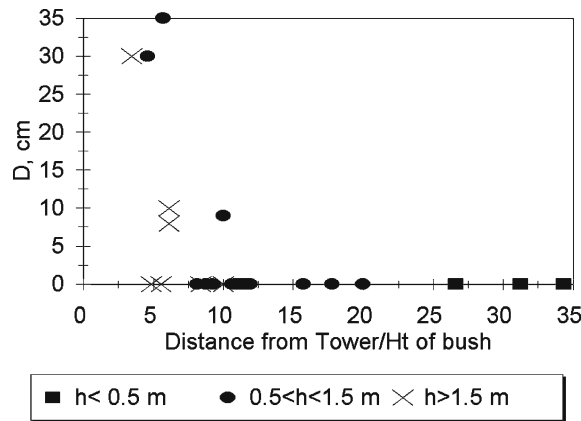


Figure 9.  $D$  versus distance upwind from the 15-m tower divided by height of the mesquite bush or mesquite coppice bush. For distance greater than 10 heights of the upwind mesquite/coppice dune,  $D$  was zero.

relationship roughly agrees with [8, 11]. In Section 4, we discuss the empirical length of protection ( $10h$ ) with the sheltering theory of Raupach [32].

#### 3.9.4. Categorization of $D$ and $z_0$ for 3-m Masts and 15-m Tower

The “Oriented” mast and tower data obtained in April 2003 were used to calculate  $D$  and  $z_0$  values. Owing to the errors in using three-point estimations of the  $D$  and  $z_0$  values, we separated the data into five rather broad categories.

- (1)  $D = 0$ ,  $z_0 < 6$  cm. We called this category “street flow.”
- (2)  $D = 0$ ,  $6 \text{ cm} < z_0 < 40$  cm. We called this category “flow affected by upstream roughness.” Taken together, categories 1 and 2 are probably the most favorable for sand flow.
- (3)  $D > 40$  cm,  $z_0 < 6$  cm. We called this category “canopy flow.”
- (4) “Separation flow” refers to the presence of reverse flow close to the ground and decelerated flow in the direction of the mean flow above the reversed flow. Transport at the lowest levels is toward the upwind bush or coppice dune. Wind direction above the reverse flow is roughly in the same direction as the 15-m mean wind direction.
- (5) “Sheltering wake flow” refers to  $0 < D < 40$  cm and  $z_0$  scattered which we interpreted to be similar to the flow exhibited by the 15-m tower data for wind directions  $114^\circ$ – $172^\circ$  when the flow was downwind from a nearby mesquite coppice dune.

Finally, we organized the nine wind locations using the five categories specified. We categorized the nine wind profile sites by the above criteria as follows for wind directions ranging between  $192^\circ$  and  $282^\circ$ :

- (a) Category 1 only: Street flow for the entire test period: Masts  $Q$  and  $D$ . Values of  $D$  for masts  $Q$  and  $D$  were always zero for winds from  $192^\circ$  to  $282^\circ$ . Data for  $z_0$  versus wind direction for masts  $Q$  and  $D$  are shown in Figure 10.
- (b) Categories 1 and 2: Intervals of street flow and intervals of flow affected by upstream roughness (mesquite): Masts  $C$ ,  $M$ ,  $N$ , and the tower.  $D$  values were almost always zero for wind directions from  $192^\circ$  to  $282^\circ$  for these masts and the tower. Figure 10 shows that masts  $C$ ,  $N$ ,  $M$  and the tower had  $z_0 > 6$  cm for part of the wind direction range from  $192^\circ$  to  $282^\circ$ . These conditions were interpreted as intervals of smooth street flow and intervals of flow affected by upwind roughness for part of the time. Figure 6 shows that the tower has “sheltering wake flow” for some wind directions outside the  $192^\circ$  to  $282^\circ$  range.
- (c) Category 3: Canopy flow for the entire test period: Mast  $P$ , which is located on top of our test dune and which is imbedded in mesquite bush. Data for  $z_0$  versus wind direction for mast  $P$  are shown in Figure 10.
- (d) Category 4: Separation flow: Mast  $O$ . We used our visual observations of a flow reversal in the 20 cm closest to the ground. The observation of flow reversal occurred for two BSNEs: D3.6 and D4.5. The BSNE sand flux collectors consist of three wind vanes that direct the sand collectors into the wind for height intervals 5–20 cm (lowest), 40–60 cm (middle) and 90–110 cm (highest). For separation flow observed for winds from  $232^\circ$  to  $282^\circ$ , the lowest BSNE vane at D3.6 indicated winds from the south (into the dune), and the lowest BSNE vane at D4.5 indicated winds from the east (into the dune). The middle and high vanes at D3.6 and D4.5 indicated wind directions similar to the wind direction at 1.5 m at mast  $O$  – about  $30^\circ$  more than the wind direction at the 15-m tower. The flow transported sediment toward the back (downwind side) of the test dune at lowest levels. Because the flow was reversed, there were insufficient data to calculate  $D$ ,  $z_0$ , or friction velocities.
- (e) Categories 5 and 2: Sheltering wake flow for part of the time; flow affected by upwind roughness for the remainder of the time: Mast  $B$ . Figure 10 shows data for mast  $B$ .

### 3.10. RATIOS OF FRICTION VELOCITY CALCULATED FROM MAST DATA TO THAT CALCULATED FROM TOWER DATA

Using the rough equality of mean wind speed at 3.15 m height (differing by less than about 10% from location to location), we used the following two qualitative rules to check the ratios of friction velocity for masts to those calculated from 15-m tower data for the same sampling times and for the condition  $D=0$ . The two rules were (1) for two locations having equal

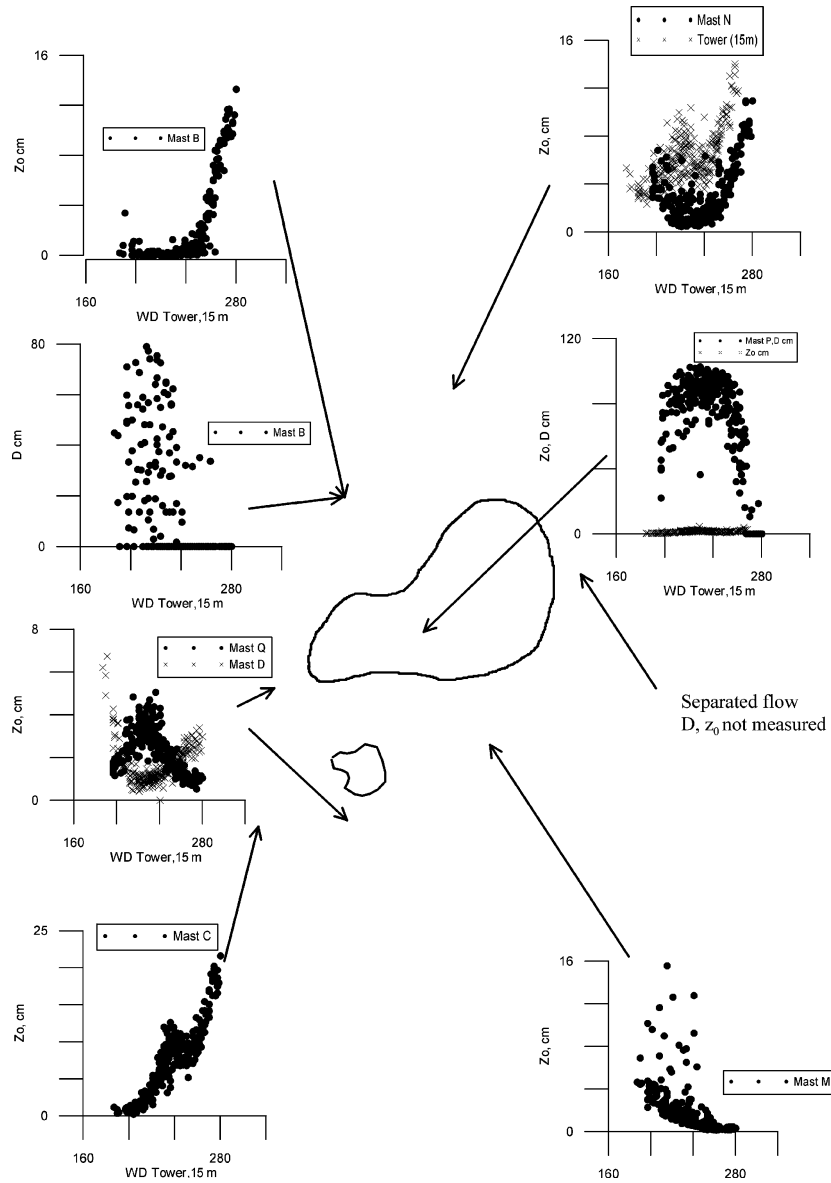


Figure 10. Three-meter mast data zero-plane displacement height  $D$  or aerodynamic roughness height  $z_0$  for “Oriented” for the month of April 2003 versus wind direction at 150-m height on the Tower. Positions of masts relative to test dune are shown by arrows. Data shown:  $z_0$  for the  $Q$  and  $D$  masts where  $D$  is zero for all wind directions;  $z_0$  for the  $C$  mast where  $D$  is zero for all wind directions;  $z_0$  for the  $M$  mast where  $D$  is zero for all wind directions;  $z_0$  for the  $N$  mast and 15-m tower where  $D$  is zero for all wind directions;  $D$  and  $z_0$  versus wind direction for the  $P$  mast atop the test dune;  $D$  for the  $B$  mast, and  $z_0$  for the  $B$  mast. For the  $O$  mast immediately downwind of the test dune, flow was separated and  $D$  and  $z_0$  could not be calculated.

$z_0$  values, the friction velocities are the same, and (2) for locations having unequal  $z_0$  values, friction velocity will be larger for the larger  $z_0$ . These two rules were validated by the data.

Figure 11 gives the ratio of friction velocity estimated at the masts to that estimated from the 15-m tower. Since the tower friction velocity is representative of a larger area and the mast friction velocity represents more localized areas, the ratio of the friction velocities shows sub-areas of the “Oriented” site that have potentially accelerated/decelerated erosion when the ratio is larger/less than one. Mast *C* has the largest ratio for friction velocities of all the masts when the wind direction at the tower is between  $240^\circ$  and  $280^\circ$ . Mast *N* also has friction velocity ratios greater than one for winds around  $200^\circ$ . Mast *B* friction velocity ratios are at a maximum for wind directions  $240^\circ$  to  $280^\circ$ , while Masts *Q* and *M* have their maxima near  $200^\circ$ . Mast *D* has friction velocities roughly 0.8 of those for the tower for the wind direction range  $200^\circ$ – $280^\circ$ . Mast *N* has roughly equal friction velocity as the tower for wind directions near  $200^\circ$  and  $280^\circ$ . The friction velocities are probably always below threshold for Mast *P* located in the mesquite growing from the test dune. The flow separation zone behind the test dune (Mast *O*) is an area of deposition, not of erosion.

### 3.11. “RANDOM”: 15-M TOWER DATA FOR $D$ AND $z_0$ VERSUS WIND DIRECTION

“Random” data for  $D$  and  $z_0$  versus wind direction for the month of April 2003 are shown in Figures 12a and 12b. Large sporadic values for  $D$  from 0 to almost 60 cm occurred for the entire range of winds faster than  $6 \text{ m s}^{-1}$  at 3 m heights. Unlike at the “Oriented” site, no range of wind directions yielded consistent patterns of  $D$ . Similarly, no pattern was seen for the  $z_0$  values versus wind direction. The  $z_0$  values varied sporadically from 2 to 6 cm. These observations suggest that the nearby smaller mesquite bushes of “Random” had similar effects for directions  $180^\circ$ – $280^\circ$  as did the “sheltering wake flow” of larger mesquite bushes at “Oriented” for directions  $112^\circ$ – $160^\circ$  (see Figure 8a and 8b). The mesquite bushes were smaller at “Random” than at “Oriented” (see Table 1) and the obvious patterns of streets at “Oriented” were absent at “Random” (see Figure 1 and 2). Finally, the larger mean optical porosity measured at “Random” (see Section 3.2) suggests that more air penetrated the smaller mesquite bushes of “Random,” leading to the chaotic pattern of  $D$  and  $z_0$  of Figure 12 compared to the well-defined streets of “Oriented” which show that  $D=0$  for large ranges of wind speed.

Figure 13 shows the values of  $z_0$  versus  $D$  for those 10-min periods when sand was moving (when  $u_* > u_{*t}$ ). Because the data of Figure 10 were all obtained while sand was moving at the site, the figure shows that the relationship obtained at our “Oriented site”; i. e., that no sand

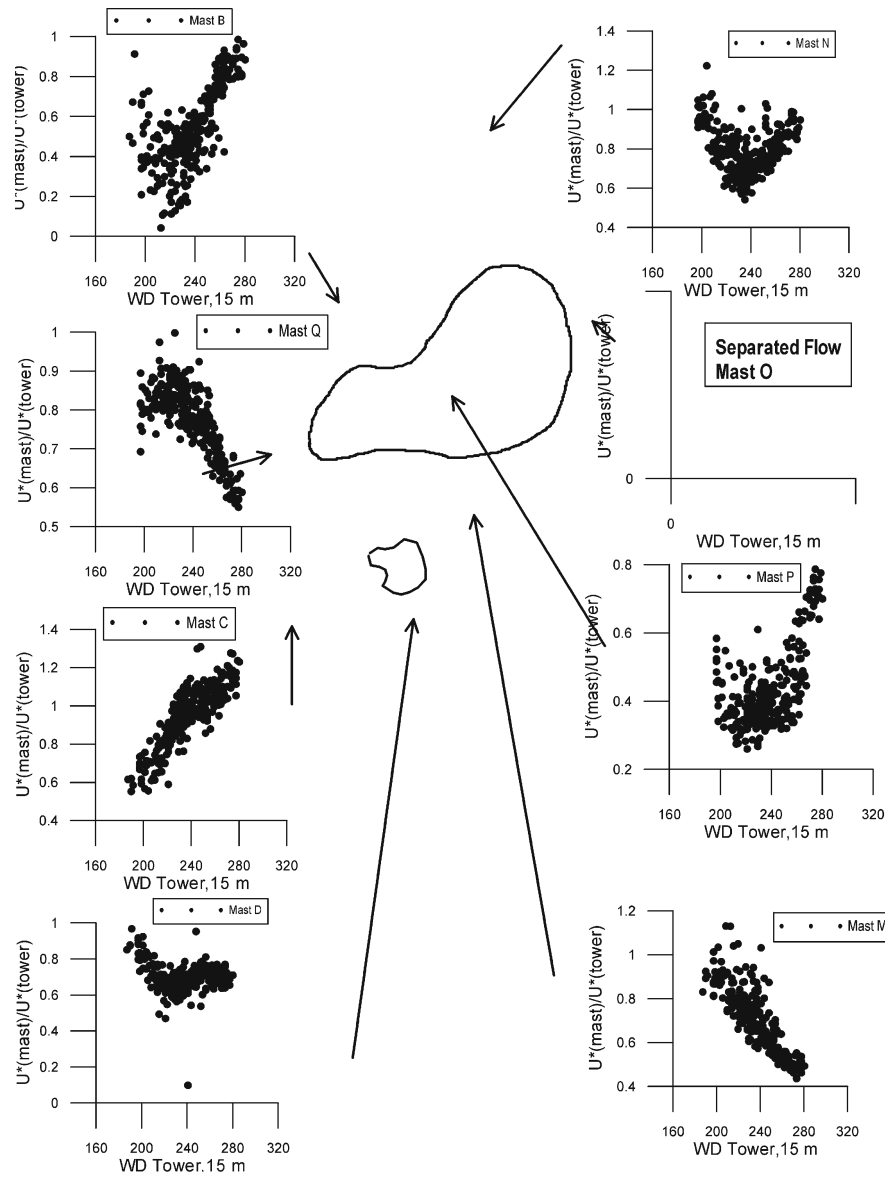


Figure 11. Three-meter mast data for 10-min friction velocity divided by 15-m tower friction velocity for the “Oriented” site for the month of April 2003 versus wind direction at 15-m height on the tower. Positions of masts relative to test dune are shown by arrows. Data for the *O* mast was not calculated since the flow showed reversal and data were insufficient to calculate friction velocity.

moved when  $D > 0$ , is not valid for the “Random” site. Therefore, use of  $D > 0$  to predict no wind erosion is only valid at sites having streets oriented with the wind direction. At the “Random” site where there are no

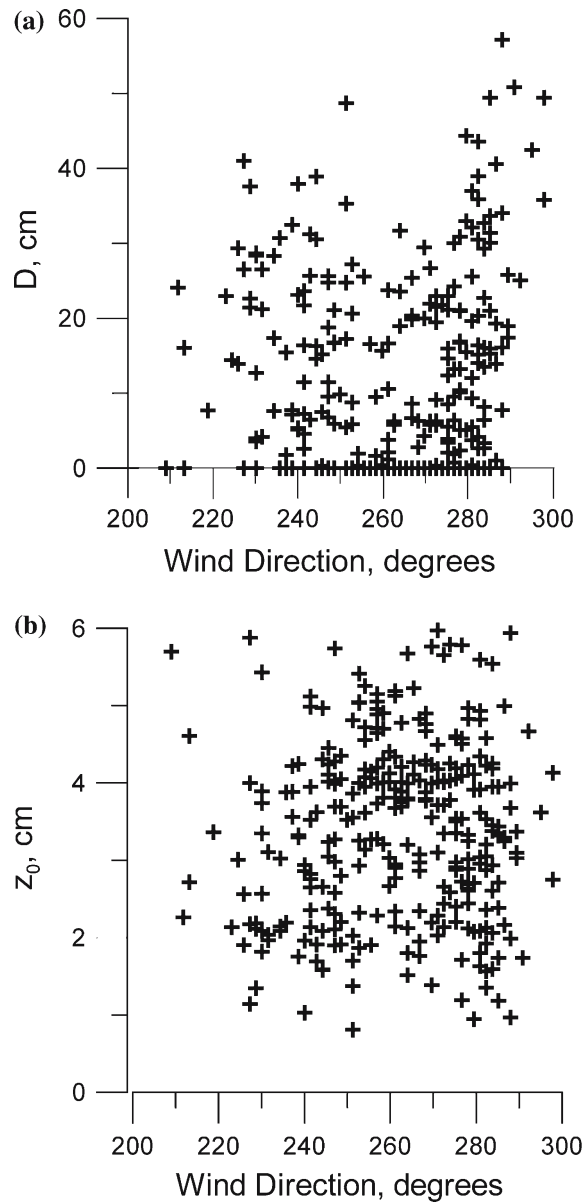


Figure 12. Data versus wind direction for the 15-m tower at the "Random" site for all our wind data for April 2003. (a) Displacement height  $D$  (cm). (b) Aerodynamic roughness height  $z_0$  (cm).

well-developed streets, there are nevertheless sand fluxes for friction velocities larger than  $100 \text{ cm s}^{-1}$ . We attribute this to chaotic and sporadic wake flow with associated chaotic sand fluxes on the narrow and short patches of bare ground between mesquite bushes at "Random."

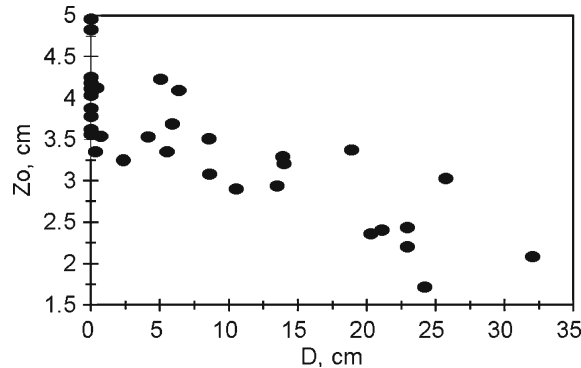


Figure 13. Aerodynamic roughness height  $z_0$  versus  $D$  for times at the “Random” site when sand movement was being detected. Note that unlike the “Oriented” site, the “Random” site can have sand motion for  $D > 0$  when the threshold friction velocity is exceeded.

### 3.12. INCREASE OF $u_*$ WITH DOWNWIND DISTANCE IN STREETS

At the “Oriented” site, connecting the positions on Figure 1 of the 3-m Masts  $C$ ,  $Q$ ,  $B$ ,  $N$  and the 15-m tower with a roughly fitted straight line showed an orientation of about  $220^\circ$ . No other combination of masts or directions yielded such a roughly fitted straight line having more than three points. After sorting our data for wind directions  $220^\circ$  to  $224^\circ$ , we found the ratios for friction velocities to the friction velocity at the tower. The mean of the ratios and standard deviation of the ratios are given in Table IV.

Masts  $C$  and  $Q$ , which are upwind of the test dune, have friction velocities comparable to that at the tower. Data for Mast  $B$  shows that  $D > 0$  for a large interval of time probably reflecting its position of being in wake flow with lower mean wind speed. The  $N$  position has  $z_0$  values smaller than at the tower that correlate with smaller friction velocities, and which may be caused by a smaller wake effect at Mast  $N$  than at the tower.

Table IV. Mean and standard deviations of ratios (friction velocities at mast to friction velocities at the 15-m tower): Data obtained in April 2003 for wind directions between  $220^\circ$  and  $224^\circ$ .

Mast:	$C$	$Q$	$B$	$N$
Mean	0.99	0.81	0.43	0.68
St. Dev.	0.09	0.05	0.13	0.10

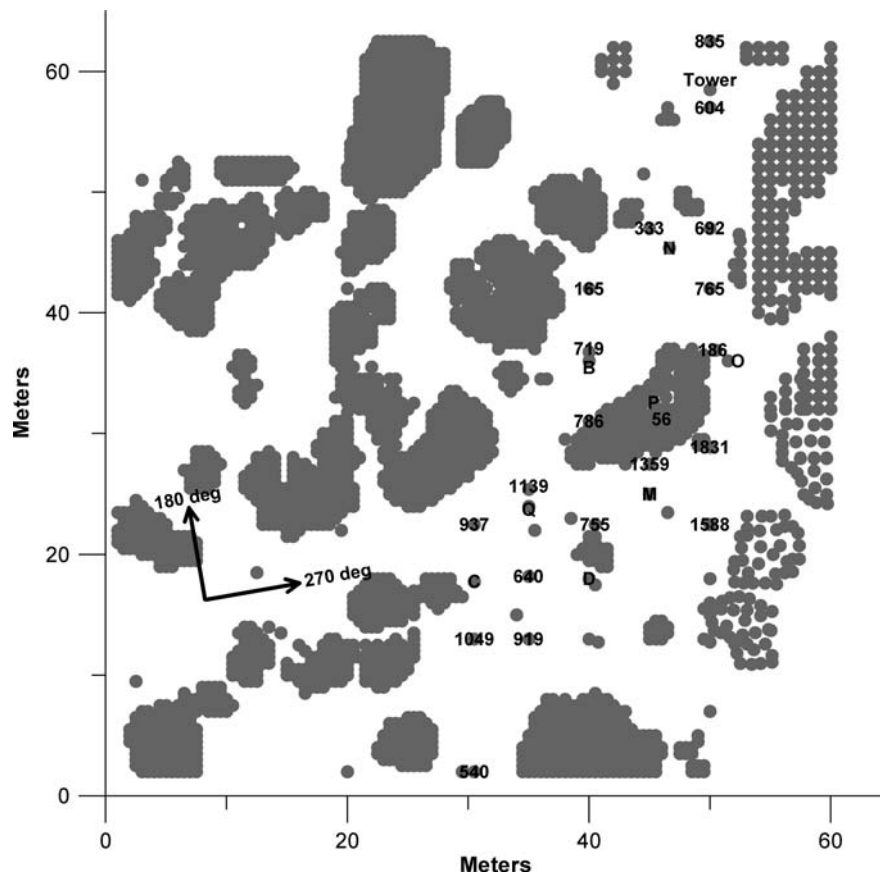


Figure 14. Accumulated sediment flux (in grams collected for the storm of April 15, 2003 per cm width of the collector opening) for locations of the collector at “Oriented.”

### 3.13. INTERPRETATION OF SAND FLUX IN “ORIENTED” AND “RANDOM” IN LIGHT OF THE ABOVE SOIL AND AERODYNAMIC PROPERTIES

Interpretations of one-day accumulations of sand fluxes at the “Oriented” site for a strong dust storm on April 15, 2003 for the sand collectors shown in Figure 1 can be made by using the five categories of aerodynamic parameters  $z_0$  and  $D$  given in Section 3.7.3. Figure 14 shows the one-day fluxes [units of  $\text{g cm}^{-1} \text{ day}^{-1}$ ] for April 15, 2003. The mean 10-min wind direction weighted by 10-min Sensit<sup>TM</sup> count for the storm of April 15 was  $252^\circ$ . The storm of April 15 was the strongest storm of April 2003. The storm began by wind speeds slightly exceeding threshold for south winds. The wind direction moved from south to west during the storm and reached the highest wind speeds for the WSW direction. The sand flows were interpreted as follows:

1. Canopy flow: the lowest flux accumulation ( $56 \text{ g cm}^{-1} \text{ day}^{-1}$ ) was collected near site *P*. Such low fluxes were expected for flow through mesquite vegetation. We expected removal of the sand by its penetration into the vegetation where more slowly moving canopy flow facilitated particle deposition.
2. Separation flow: the third lowest accumulation ( $186 \text{ g cm}^{-1} \text{ day}^{-1}$ ) was collected near site *O*, a separation zone behind the test dune. This location was in a protected zone of the “Oriented” site where deposition of sand was expected to be caused by the reversed flow directing sand flow into the more slowly moving air at the back of the dune.
3. The second-highest accumulation of the nine mast and tower locations was near Mast *Q*, which was categorized as “street flow.” The accumulation was  $1139 \text{ g cm}^{-1} \text{ day}^{-1}$ .
4. The highest accumulation close to a mast location was  $1359 \text{ g cm}^{-1} \text{ day}^{-1}$  at Mast *M*. The category of this collector was street flow part of the time and flow affected by upstream roughness (mesquite) the remainder of the time. Because the strongest winds were in the “unrestricted flow” part of this category, strong sand flow was collected near Mast *M*. This location also was near the boundary of a dune with a street where large fluxes of sand were carried.
5. The collector near Mast *B* was indicated medium-levels of sand flux ( $719 \text{ g cm}^{-1} \text{ day}^{-1}$ ). This was expected since it was in a protected region during the first half of the storm and in an active region during the second half of the storm. The collector 5 m north of Mast *B* had the second-lowest collection, indicating that it was in a protected area for most of the storm.

At “Random,” Figure 9a shows that wind directions between  $180^\circ$  and  $280^\circ$  indicated site *D* was be sporadically zero to almost 60 cm. All sand flow was sporadic and turbulent. The “Random” flow did not move as much sand as at “Oriented,” where established streets led to an organized sand flow in the direction of the street. Figure 15 shows sand collectors at “Random” on April 15, 2003 collected less sand on average and without the patterns observed at “Oriented.” This is consistent with the results [1] that “Random” mass fluxes were consistently lower compared to “Oriented” fluxes during the windy season for several years.

#### 4. Discussion

We used the data from the 15-m tower at the “Oriented” site to compare with Raupach’s [32] formula of the length of the protected area sheltered by a plant. This area had the approximate width of the plant and length  $L$  downwind of the plant

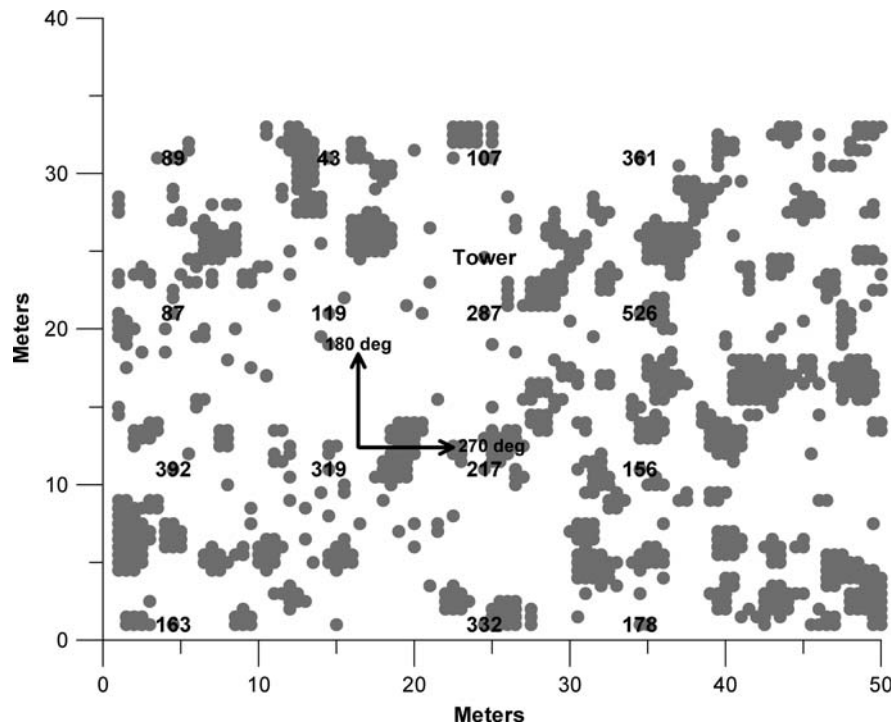


Figure 15. Accumulated sediment flux (in grams collected for the storm of April 15, 2003 per cm width of the collector opening) for locations of the collector at "Random".

$$L = h \frac{U(h)}{u_*}, \quad (5)$$

where  $h$  is the height of the plant/coppice dune,  $U(h)$  is the wind speed just above the plant/coppice dune, and  $u_*$  is the friction velocity. Using height  $h$  of the second anemometer (approximately 2.6 m) along with measured  $U(h)$  and  $u_*$  values, the mean of  $U(2.6\text{ m})/u_*$  was  $9.3 \pm 0.9$  for all the 2003 wind data. This value is quite close to our empirical finding that beyond 10 h, the zero-plane displacement heights were zero. Thus, our measurements support the theory of Raupach.

These results have important implications for those attempting to remediate grasslands that have been invaded by mesquite, particularly where streets have begun to form. They are also important for modeling the airflow within mesquite dune lands [33] because they can provide data with which to compare model results. Because mesquite plants are likely to retain their aerodynamic effects long after they have been killed by herbicides, initial plant establishment should be concentrated in those areas where sand fluxes are predicted to be lowest.

## 5. Conclusions

Comparisons of 15-m-tower wind directions ranging from roughly south to west and 1.5-m wind directions from the 3-m masts show steering of wind by the mesquite bushes (roughness elements) for the "Oriented" site. The steering increases the 1.5-m mast wind directions relative to 15-m tower direction for tower wind directions from  $195^\circ$  to  $220^\circ$  for five of the eight mast locations; for these mast locations the wind direction at the mast is seen to agree with the 15-m tower wind direction for at least one wind direction in the south to west quadrant.

For the "Oriented" site that had obvious streets (unobstructed bare soil elongated in the direction of strongest winds) aerodynamic parameters  $z_0$  and  $D$  were used to identify zones where sand movement would be unrestricted or inhibited. The data showed that large parts of the two streets north and south of the test dune have zero  $D$  values and  $z_0$  values smaller than 6 cm (category 1). These areas have the largest sand fluxes. For a limited range of wind direction at the 15-m tower near  $220^\circ$  (moving up the middle of the street north of the test dune), friction velocities increase (on the average) with distance from the nose of the test dune to the tower. Locations embedded in mesquite bushes have values of  $D$  much larger than zero; sand fluxes here are small fractions of sand movement rates in streets. For downwind distances that are within about two heights of the upwind coppice dune, there is a zone of separation flow where the reversal of wind movement in the lowest 20 cm corresponds to a negative sand flux. In magnitude, this flux is a small fraction of that in streets as a result of lower wind velocities. For a downwind distance from the coppice dune of about two heights of the dune to a distance roughly 10 heights of the dune, there is a zone of protection where sand fluxes are small fractions of that for category 1. These zones were observed to have non-zero  $D$ . For distances greater than about 10 to 15 times the dune height, the values for  $D$  are zero, but values of  $z_0$  are considerably larger than 5 cm (category 2). This pattern suggests the wake-influenced flow similar to that identified by Walker and Nickling [11]. Locations that have this kind of flow did have medium to large sand fluxes, in spite of the correlation of larger  $z_0$  values with larger threshold friction velocities [16]. Beyond a distance of 15 to 20 dune heights for flat soil, the  $z_0$  values are of the order 2–5 cm.

The "Random" site had poorly developed streets. Flows for all wind directions tested at "Random" were sporadic and chaotic; sand flow (if there was any) was smaller in total flux than that at "Oriented." Part of "Random" air flow is probably caused by wind blowing through the more porous mesquite bushes of "Random" compared to those at "Oriented." "Oriented" also had more coppice dune development than "Random." We attribute the differences in sand flux at "Oriented" compared to "Random"

to be a consequence of well-developed streets with unrestricted flow for some wind directions and wind speeds at "Oriented," and highly turbulent and sporadic flow on the undeveloped streets at "Random."

A summary of our findings follows:

- (1) Mesquite streets having  $D = 0$  and  $z_0 < 6$  cm for all times in a given wind direction can be associated with large fluxes of sand.
- (2) Mesquite streets having  $D = 0$  and  $z_0 > 6$  cm for all times in a given wind direction have sand movement partially affected by upwind roughness. This roughness results from mesquite bushes or mesquite coppice dunes that are upwind for distances between 10 and 20 heights of the dune or bush. Fluxes in this flow can be large.
- (3) Locations that are imbedded in mesquite bushes  $D$ s are greater than 0 and reach values of about 1 m. For these locations, sand movement rates are a small fraction of the sand movement rates in streets.
- (4) In zones that are immediately downwind of mesquite bushes or coppice bushes, there is separation flow where sand fluxes are a small fraction of those in streets and are reversed in direction.
- (5) Farther downwind of mesquite plants to a distance roughly 10 times the height of the mesquite plant, there is a zone of non-zero  $D$  where fluxes are reduced compared to those in streets.

## 6. Disclaimer

The research presented here was performed under the Memorandum of Understanding between the U. S. Environmental Protection Agency (EPA) and the U. S. Department of Commerce's National Oceanic and Atmospheric Administration (NOAA) and under agreement number DW12921548. This work reflects a contribution to the NOAA Air Quality Program. Although it has been reviewed by EPA and NOAA and approved for publication, it does not necessarily reflect their policies or views.

## Acknowledgments

The authors are pleased to acknowledge Messrs. Jim Lenz and David Thatcher for securing the wind data. Mention of trade names or commercial products does not constitute endorsement or recommendation for use. This research was carried out as part of the LTER program at the Jornada del Muerto site. The Jornada LTER project is administered by Duke University and is supported by National Science Foundation grant DEB94-11971.

## Endnote

<sup>1</sup>Names of commercial products imply no endorsement by the authors or the U. S. Department of Commerce.

## References

1. Gillette, D. and Pitchford, A.: 2004, Sand flux in the northern Chihuahuan Desert, New Mexico, USA, and the influence of mesquite-dominated landscapes, *J. Geophys. Res.* **109**, F04003, doi:10.1029/2003JF000031.
2. Musick, H.B. and Gillette, D.A.: 1990, Field evaluation of relationships between a vegetation structural parameter and sheltering against wind erosion, *Land Degradation and Rehabilitation* **2**, 87–94.
3. Raupach, M.R., Gillette, D.A. and Leys, J.F.: 1993, The effect of roughness elements on wind erosion threshold, *J. Geophys. Res.* **98**, 3023–3029.
4. Wyatt, V. and Nickling, W.G.: 1997, Drag and shear stress partitioning in sparsely vegetated desert canopies, *Earth Surf. Processes Landforms* **21**, 607–620.
5. Lancaster, N. and Baas, A.: 1998, Influence of vegetation on sand transport by wind: Field studies at Owens Lake, California, *Earth Surface Processes and Landforms* **23**, 69–82.
6. Grant, P.F. and Nickling, W.G.: 1998, Direct field measurements of wind drag on vegetation for application to windbreak design and modeling, *Land Degradation and Development* **9**, 57–66.
7. Gillies, J.A., Lancaster, N., Nickling, W.G. and Crawley, D.M.: 2000. Field determination of drag forces and shear stress partitioning effects for a desert shrub (*Sarcobatus vermiculatus*, greasewood). *J. Geophys. Res. Atmospheres* **105** (D20): 24871–24880.
8. Frank, A. and Kocurek, G.: 1996, Airflow up the stoss slope of sand dunes: Limitations of current understanding, *Geomorphology* **17**: 47–54.
9. Lancaster, N., Nickling, W.G., McKenna Neuman, C. and Wyatt, V.: 1996, Sediment flux and airflow on the stoss slope of a barchan dune, *Geomorphology* **17**, 55–62.
10. Nickling, W.G. and McKenna Neuman, C.: 1999, Recent investigations of airflow and sediment transport over desert dunes, In: A. Goudie, I. Livingstone and S. Stokes (eds.), *Aeolian Environments and Landforms*, Wiley and Sons, Chichester.
11. Walker, I.J. and Nickling, W.G.: 2002, Dynamics of secondary airflow and sediment transport over and in the lee of transverse dunes, *Progress in Physical Geography* **26**, 47–75.
12. Gillette, D. and Chen, W.: 2001, Particle production and aeolian transport from a “supply-limited” source area in the Chihuahuan Desert, United States, *J. Geophys. Res.* **106** (D6): 5267–5278.
13. Raupach, M.R., Woods, N., Dorr, G., Leys, J. and Cleugh, H.: 2001, The entrapment of particles by windbreaks, *Atmos. Environ.* **35**, 3373–3383.
14. Lumley, J.L. and Panofsky, H.A.: 1964, *The Structure of Atmospheric Turbulence*, John Wiley and Sons, New York, 239 pp.
15. Arya, S.P.: 1999, *Air Pollution Meteorology and Dispersion*, Oxford University Press, Oxford, 310 pp.
16. Marticorena, B., Bergametti, G., Gillette, D. and Belnap, J.: 1997, Factors controlling threshold friction velocity in semi-arid and arid areas of the United States, *J. Geophys. Res.* **102**, 23, 277–23, 287.
17. Bagnold, R.A.: 1941, *The Physics of Blown Sand and Desert Dunes*, Methuen and Co., London, 265 pp.
18. Owen, P.R.: 1964, Saltation of uniform grains in air, *J. Fluid Mech.* **20**, 225–242.
19. Iversen, J.D. and White, B.R.: 1982, Saltation threshold on Earth, Mars and Venus, *Sedimentology* **29**, 111–119.
20. Marticorena, B. and Bergametti, G.: 1995, Modeling the atmospheric dust cycle: 1. Design of a soil-derived dust emission scheme, *J. Geophys. Res.* **100**, 16,415–416,430.

21. Stockton, P. and Gillette, D.A.: 1990, Field measurement of the sheltering effect of vegetation on erodible land surfaces, *Land Degradation and Rehabilitation* **2**, 77–85.
22. Gillette, D., Herbert, G., Stockton, P. and Owen, P.: 1996, Causes of the fetch effect in wind erosion, *Earth Surface Processes and Landforms* **21**, 641–659.
23. Gillette, D.A., Hardebeck, E. and Parker, J.: 1997, Large-scale variability of wind erosion mass flux rates at Owens Lake, 2, Role of roughness change, particle limitation, change of threshold friction velocity, and the Owen effect, *J. Geophys. Res.* **102**, 25989–25998.
24. Pasquill, F.: 1962, *Atmospheric Diffusion*, Van Nostrand, London, 297 pp.
25. Miller, I. and Freund, J.F.: 1977, *Probability and Statistics for Engineers, Second Edition*, Prentice-Hall, Inc., Englewood Cliffs, New Jersey, 529 pp.
26. Priestley, C.H.B.: 1959, *Turbulent Transfer in the Lower Atmosphere*, University of Chicago Press, Chicago, 130 pp.
27. Kaimal, J.C. and Finnigan, J.J.: 1994, *Atmospheric Boundary Layer Flows, Their Structure and Measurement*, Oxford, New York, 289 pp.
28. Riehl, H.: 1954, *Tropical Meteorology*, McGraw Hill, New York, 392 pp.
29. Gee, G.W. and Bauder, J.W.: 1986, Particle-size analysis. In: Klute, A. (Ed.), *Methods of Soil Analysis. Part I. Second Edition*, pp. 383–411. ASA and SSSA, Madison, WI, 1888 pp.
30. Buckman, H.O. and Brady, N.C.: 1970, *The Nature and Properties of Soils, Seventh Edition*, Macmillan Company, London, 653 pp.
31. Helm, P.J. and Breed, C.S.: 1999, Instrumented field studies of sediment transport by wind, in C. S. Breed and M. C. Reheis, *Desert Winds: Monitoring Wind-Related Surface Processes in Arizona, New Mexico, and California*, U. S. Geological Paper 1598, U. S. Gov. Printing Office, Washington DC, 29–51.
32. Raupach, M.R.: 1992, Drag and drag partition on rough surfaces. *Boundary-Layer Meteorology* **60**, 375–395.
33. Bowker, G.E., Gillette, D.A., Bergametti, G. and Marticorena, B.: Modeling flow patterns in a small area in the northern Chihuahuan desert using QUIC (Quick Urban & Industrial Complex), *Environmental Fluid Mech.*